CHAPTER 2

LINEAR INTERNAL WAVES

Natural bodies of fluid such as the atmosphere, the oceans and lakes are characteristically stably stratified: that is, their mean (potential) density decreases as one goes upwards, in most regions and for most of the time. When they are disturbed in any way, internal waves are generated. These ubiquitous motions take many forms, and they must be invoked to explain phenomena ranging from the temperature fluctuations in the deep ocean to the formation of clouds in the lee of a mountain. In this chapter we summarize the results which can be obtained using linear theory (i.e. when the amplitudes are assumed to be small), and in §3.1 extend some of them to describe waves of large amplitude.

Many of the elementary properties of infinitesimal wave motions in stratified fluids can be introduced conveniently by considering waves at an interface between two superposed layers, and so this case is treated first in §2.1. These waves are analogous to waves on a free water surface, and therefore seem very familiar. It should be emphasized at the outset, however, that they are *not* the most general wave motions which can occur in a continuously stratified fluid. Energy can propagate through such a fluid at an angle to the horizontal, not just along surfaces of constant density, and our intuition based on surface waves is of little help here. The more general theory, and a comparison between the two descriptions, is given in §2.2.

2.1. Waves at a boundary between homogeneous layers

Consider two superposed layers, each of which has constant density ρ_0 and $\rho_1 = \rho_0 + \rho'$ say and is initially at rest. Only two-dimensional waves will be allowed, with motions confined to the x, z plane (z positive upwards) and crests consisting of parallel ridges running in the y-direction. Waves of this kind are easily set up in a laboratory

channel (see fig. 2.1 pl. 1)†, and more general three-dimensional disturbances can be treated by superimposing such motions (because the equations are linear when the motions are kept small). The fluid will be assumed inviscid in these introductory sections, and viscous effects added where they are needed to explain particular phenomena. For the derivation of the results quoted here, reference should be made to Lamb (1932, ch. 9).

The linearized equations (1.3.8) can be applied to each of the layers separately, with ρ constant. *Within* the layers the motion is irrotational and so potential theory can be used to describe the flows above and below the interface. The equations satisfied by the velocity potentials (which are defined by $u = -\partial\phi/\partial x$, $w = -\partial\phi/\partial z$ and because of the continuity equation satisfy $\nabla^2\phi = 0$ in each layer) are obtained by integrating the component equations of (1.3.8). They are

$$\left.\begin{aligned} \frac{p_0}{\rho_0} &= \frac{\partial\phi_0}{\partial t}, \\ \text{and} \qquad \frac{p_1}{\rho_1} &= \frac{\partial\phi_1}{\partial t} - g\frac{\rho'}{\rho_1}z. \end{aligned}\right\} \tag{2.1.1}$$

These equations apply whatever the (small) motion in the two layers, but we can simplify the discussion by considering just one component of a Fourier decomposition, a sinusoidal travelling wave which displaces the interface an amount

$$\eta = a \exp \mathrm{i}(kx - \omega t), \tag{2.1.2}$$

(where k is a wavenumber and ω is the angular frequency). Clearly η and ϕ must be related by $\partial\eta/\partial t = -\partial\phi/\partial z$, since these are alternative expressions for the vertical velocity. The form of solution also depends on the boundary condition away from the interface, and two important cases are treated separately below.

2.1.1. *Progressive waves in deep water*

Suppose first that the layers are both very deep compared with the wavelength, so that the disturbances vanish at $kz = \pm\infty$, where the

† The plates are to be found between p. 96 and p. 97.

origin of z is at the interface. Velocity potentials satisfying (2.1.1) and the boundary conditions (2.1.2) and at infinity are

$$\left.\begin{aligned}\phi_0 &= A_0 e^{-kz} \exp i(kx-\omega t),\\ \phi_1 &= A_1 e^{kz} \exp i(kx-\omega t).\end{aligned}\right\} \tag{2.1.3}$$

The displacement η must be the same in the two layers, so

$$kA_0 = -kA_1 = i\omega a. \tag{2.1.4}$$

A second condition relating the constants A_0 and A_1 is that the pressure must be continuous at the interface (provided no extra forces are introduced by surface tension). For these to be consistent, there must be a special relation between ω and k (the dispersion relation) which can be expressed in terms of the phase velocity $c = \omega/k$ and the wavelength $\lambda = 2\pi/k$ as

$$c^2 = \frac{g}{k}\frac{\rho'}{\rho_0+\rho_1} = \frac{g\lambda}{2\pi}\frac{\rho_1-\rho_0}{\rho_1+\rho_0}. \tag{2.1.5}$$

Such waves are called *dispersive*, because motions generated with given frequency but different wavelengths move at different velocities and will separate as they travel away from the source. For example if the oceanic thermocline is disturbed in an arbitrary way, the longest waves generated will always be the first to reach a distant observing point.

As with all gravity waves, the energy is divided between the kinetic and potential forms, the two contributions being equal when averaged over a wavelength. The phase velocity c (which will sometimes be written c_p) is reduced by the factor

$$[\rho'/(\rho_0+\rho_1)]^{\frac{1}{2}}$$

compared with that for surface waves. In typical situations in the ocean, for example, where $\rho'/\rho_0 \approx 10^{-3}$, internal waves travel with only a few per cent of the velocity of surface waves. Energy is propagated along the interface with the group velocity

$$c_g = \frac{d\omega}{dk} \tag{2.1.6}$$

which in this case is just $c_g = \frac{1}{2}c$, a relation which also holds for surface waves on deep water. Fluid particles move in paths which

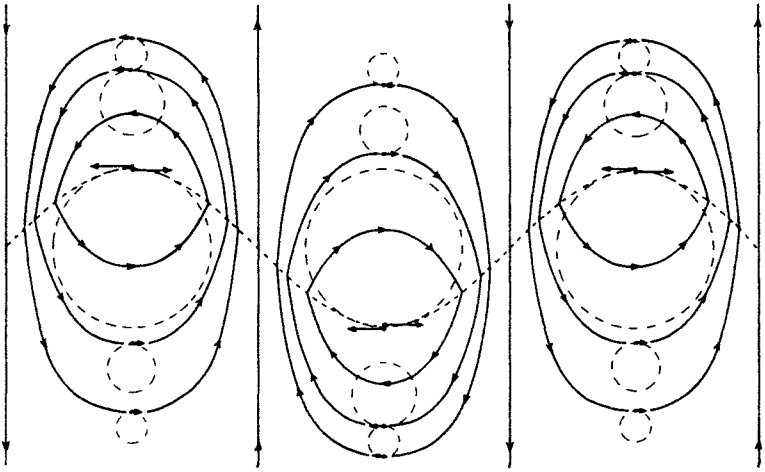

Fig. 2.2. Streamlines and orbits in a progressive internal wave travelling from left to right along the interface between two fluids. From Defant (1961).

(in the linear approximation) are circular, with amplitude decreasing exponentially with distance from the interface. (See fig. 2.2.)

The solutions (2.1.3) are consistent with the general rotational property of stratified motions (§ 1.3). Although the normal velocity has been made continuous, (2.1.4) shows that the tangential velocity changes sign across the interface. The potential flows in two layers are separated by a vortex sheet, with a maximum shear at the crests and troughs of the waves. In a real fluid, of course, such discontinuities will be spread out by viscosity into a vortex layer of finite thickness. With miscible fluids in the two layers (the case we will be most concerned with) diffusion of the property producing the density difference (i.e. heat or salt) will already have produced a continuous density distribution rather than strictly a step, and this will modify the vorticity distribution associated with the wave even without viscosity (cf. § 4.3.3). There will always be a maximum shear where the density gradient is a maximum. (See, for example, Phillips 1966*a*, p. 168.)

2.1.2. *Waves between layers of finite thickness*

More general boundary conditions can be put on (2.1.1), with (2.1.2) again applied at the interface. When the fluids are confined between rigid horizontal planes at $z = h_0$ and $z = -h_1$ so that $w = 0$ at these depths, the dispersion relation becomes

$$c^2 = \frac{g\rho'}{k}(\rho_0 \coth kh_0 + \rho_1 \coth kh_1)^{-1}. \tag{2.1.7}$$

Various special cases are recovered using the limits $\coth kh \to 1$ as $kh \to \infty$ (which when kh_0 and kh_1 are both large gives (2.1.5)), and $\coth kh \to (kh)^{-1}$ as $kh \to 0$. When kh_0 is large and kh_1 is small, the phase velocity is

$$c^2 = \frac{\rho'}{\rho_1} g h_1. \tag{2.1.8}$$

Small amplitude *long* waves on a layer of denser fluid underlying a deep light fluid are thus *non-dispersive*. Their phase velocity depends on the layer depth and the densities (through a reduced acceleration) but not on the wavenumber, and $c_g = c$. In this limit the vertical acceleration may be neglected (a result which continues to be valid for *finite* amplitude long waves – see §3.1.1), and the horizontal velocity is the same for all particles on a vertical line. This implies that a line of dye just moves back and forth as the wave passes by; the amplitude of the vertical velocity increases linearly from zero with distance above the solid bottom.

When there is a free surface above the upper layer the boundary condition to be applied there is more complicated; this case will be considered only to the extent needed to show how the internal wave motions may be affected. Because of the extra degree of freedom, the dispersion relation is now a quadratic in c^2; for each k, two different wave modes may exist. If one now adds the Boussinesq approximation (for the first time in this chapter restricting the density variation), it can be shown that the extra root is approximately

$$c_1^2 = \frac{g}{k} \tanh k(h_0 + h_1), \tag{2.1.9}$$

and c_2^2 is of the form (2.1.7). The first wave (the 'barotropic' mode) is identical with a surface wave on a layer of constant density with

depth (h_0+h_1). It has particle velocities decreasing with depth in the same way, with no discontinuity of tangential velocity at the internal boundary, and this remains true of the *surface* mode for an arbitrary distribution of density with depth.

The second mode with phase velocity c_2 is the internal wave, with largest amplitude and a discontinuity in u at the interface. Just below the free surface is a level where the motions vanish, and the phase of the displacements at the surface is opposite to that at the interface. The horizontal velocity u at the surface can be large, and regions of maximum convergence of u lie above the nodes of the interface displacement. The resulting gathering of contaminants (or some other process which changes the reflectivity at a convergence) can produce visible lines or 'slicks' which are an indication of the presence of two-dimensional internal waves (La Fond 1962, and see fig. 2.3 pl. IV). The vertical displacement of the free surface is smaller than that at the interface by a factor of the order $-\rho'/\rho_0$; for many geophysical applications this is negligible, and the surface can be treated as a rigid lid as far as the internal waves are concerned.

This last statement can, however, be turned round the other way: because of the much smaller potential energy changes needed to produce an internal wave, *imposed* disturbances at the surface can be very effective generators of internal waves. The phenomenon of 'dead water', an increased resistance to the motion of a ship when it is steaming on a thin light surface layer overlying denser water, can be explained in this way, as was shown in a classic series of experiments by Ekman (1904). So long as the speed is less than $c = (g'h_0)^{\frac{1}{2}}$ there will be an extra drag due to an internal wave which moves with the ship, but if the speed can be increased beyond this value, only the surface mode can be generated and the drag is much reduced.

2.1.3. *Standing waves*

The properties of internal standing waves, in which sections of an interface oscillate vertically between fixed nodes, can be derived by superimposed identical wavetrains travelling in opposite directions, and few specific results need be quoted here. There is more to be said about the finite amplitude case (§3.1.1) but we should note one result which is used in §4.3.2: the maximum shear occurs now at the

nodes i.e. the position of maximum slope (instead of at the crests and troughs as for progressive waves). The second wavetrain can be formed by reflection of a travelling wave from a solid barrier, and so standing waves (called surface or internal seiches) are of interest especially in closed basins such as lakes. One is thus led to study the free modes of vibration for various density distributions and basin shapes, solving an eigenvalue problem to determine the normal modes and associated resonant periods.

In the simplest case of longitudinal oscillations of two layers contained in a rectangular basin which is narrow but much longer than its depth, the long wave approximation is appropriate for the first few modes, the relevant wavelength for the seiche with one nodal line being twice the length of the lake. The two-layer approximation is often a good one here, since typical observations in lakes (or the ocean) show a well-mixed warm surface layer separated from a colder homogeneous region by a shallow *thermocline*, or layer of high gradient. The periods of all the internal seiches of this kind are (cf. (2.1.7))

$$T = \frac{2l}{n}\left(g\frac{\rho'}{\rho_0}\frac{h_0 h_1}{h_0+h_1}\right)^{-\frac{1}{2}}, \tag{2.1.10}$$

where n is the number of nodal lines. The motions are predominantly horizontal and of opposite sign above and below the interface, and again the vertical displacements at the surface are smaller than those at the interface by a factor ρ'/ρ_0, with opposite senses of tilt at these two levels.

A seiche can be set up by wind blowing along a lake, which piles surface water up at the leeward end. At the same time the bottom layer comes closer to the surface to windward, driven by a horizontal pressure gradient in the opposite direction to that in the surface layer, and it may even reach the surface there (see fig. 2.4). This quasi-steady state (which when the wind drops leads to the seiches) is complicated by the return circulations set up in each of the layers. It should be noted too that seiches set up in this way can be of such large amplitude that non-linear theory must be used to give a full description of them (cf. §3.2.2); a particularly good example in Loch Ness has been studied recently by Thorpe, Hall and Crofts (1972).

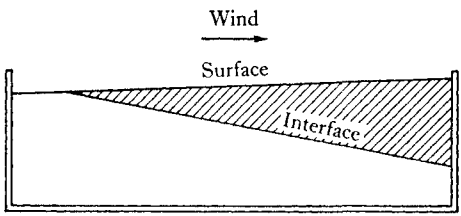

Fig. 2.4. The mechanism of generation of an internal seiche.

Proudman (1953) has shown how such calculations can be extended to basins of variable width, and to those in which the transverse oscillations must also be considered. Cases where there are several superposed layers, rather than just two, are also little different in principle, with another period and associated mode of oscillation in the vertical becoming possible each time a layer is added. For example, Mortimer (1952) obtained good agreement between observed and computed periods of internal oscillations in Lake Windermere by approximating to the density distributions using three layers. As discussed in chapters 8 and 10, step-like distributions are often observed even in large bodies of stratified fluid (such as the ocean), and the multi-layer wave theory will also be relevant there. When the lowest modes dominate, of course, the motions will be little affected by the presence of thin layers, though the microstructure will influence measurements of temperature fluctuations made at fixed depths (Phillips 1971, Garrett and Munk 1971).

When the density distribution becomes truly continuous, an infinite set of modes becomes possible and this leads us to the subject of the next section, where a simple example is given. A method of practical computation of modes for an arbitrary density distribution was developed by Fjeldstad (1933), but neither this nor more recent work on this problem will be described here.

2.2. Waves in a continuously stratified fluid

Infinitesimal motions in a continuously stratified incompressible fluid, otherwise at rest, are described by (1.3.1), (1.3.2) and (1.3.8), in which arbitrarily large variations of mean density with height are

retained, but the non-linear terms are neglected because they are products of two small quantities. For two-dimensional motions, the component equations can be written as

$$\left.\begin{aligned} \frac{\partial u}{\partial t}+\frac{1}{\rho}\frac{\partial p'}{\partial x} &= 0,\\ \frac{\partial w}{\partial t}+\frac{1}{\rho}\frac{\partial p'}{\partial z}+g' &= 0,\\ \frac{\partial u}{\partial x}+\frac{\partial w}{\partial z} &= 0,\\ \frac{\partial g'}{\partial t}-N^2 w &= 0, \end{aligned}\right\} \qquad (2.2.1)$$

where $\rho = \rho(z)$ (now assumed to be continuous), and N, defined by

$$N^2 = -(g/\rho)(\partial\rho/\partial z),$$

is the buoyancy frequency. The fourth equation indicates that density variations at a fixed point are due entirely to the vertical displacement, and are 90° out of phase with the vertical velocity.

Two complementary approaches to this problem are instructive and we will first consider the one which emphasizes the similarity with the problem of waves in layered fluids.

2.2.1. *Description in terms of modes*

Various forms of equations for velocity components or a stream-function can be obtained from the above set by the successive elimination of the variables; one such reduction will be made in §2.2.2 after adding the restriction of the Boussinesq approximation, but this is not a necessary restriction. It is already clear that wave-like solutions of (2.2.1) are possible, with u, w, p', and g' depending on time through a factor $e^{i\omega t}$. An especially simple form of solution has been obtained for the case of an exponential density distribution, say

$$\rho = \rho_s e^{-z/H} \qquad (2.2.2)$$

(which gives $N^2 = g/H$, a constant), since exponential factors can

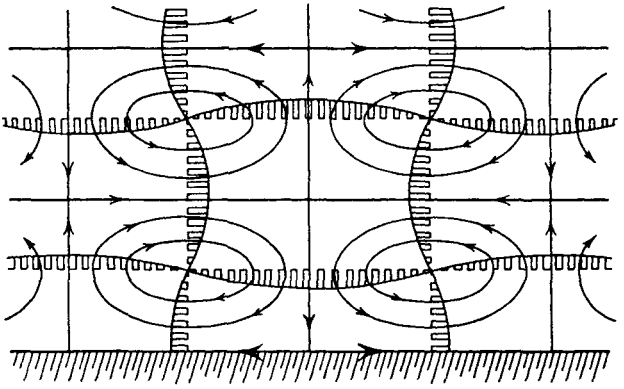

Fig. 2.5. Displacements and streamlines in a cellular standing internal gravity wave. (From Prandtl 1952.)

appear in each of the other terms. Only the velocity components are written down here following Prandtl (1952):

$$\left.\begin{aligned} u &= a\omega\, e^{z/2H} \cos kx \left(\frac{1}{2Hk}\cos mz - \frac{m}{k}\sin mz\right) e^{i\omega t}, \\ w &= a\omega\, e^{z/2H} \sin kx \cos mz\, e^{i\omega t}, \end{aligned}\right\} \qquad (2.2.3)$$

where a is the (small) amplitude, and the real part is implied in each case. The associated pattern of displacements is drawn in fig. 2.5.

These expressions represent a cellular standing wave, with horizontal and vertical wavelengths $\lambda_h = 2\pi/k$ and $\lambda_v = 2\pi/m$ which are twice the distance between the nodal lines (i.e. twice the width or height of the cells shown). The close correspondence with the modal description of waves on layers is evident; this pattern can be fitted in a closed rectangular region whose boundaries coincide with the planes of no normal motion, and there can be an arbitrary number of cells in the horizontal and vertical. The cells are identical in size, but the amplitude increases upwards in such a way that the energy (proportional to $\rho(u^2+w^2)$) is the same in each. This is a particular example of the result quoted in §1.3; the velocity is increased by a factor $(\rho_s/\rho)^{\frac{1}{2}}$ compared with that calculated by assuming small variations of density (small z/H). There is a definite frequency associated with each mode, namely

$$\omega = N\left(\frac{k^2}{k^2+m^2+1/4H^2}\right)^{\frac{1}{2}}. \qquad (2.2.3a)$$

In the limit where H or the scale height H_s are large, the same form of result applies to gravity waves in an isothermal compressible atmosphere (another case of an exponential density variation), but in the compressible case $N^2 = [(\gamma - 1)/\gamma](g/H_s)$ (see (1.2.5)).

Internal standing waves with a variety of modal structures have been produced in a laboratory tank by Thorpe (1968*a*), and several of these are illustrated in fig. 2.6 pl. 1. The bands of colour are merely markers in a continuous density gradient, which bring out clearly the property common to this and stepped structures, namely the vertical oscillation of density surfaces (in phase over the whole of a cell for standing waves).

2.2.2. *Description in terms of rays*

We now turn to the second way of describing internal wave motions in a fluid with continuous stratification. Though this can be shown to be entirely equivalent to the mode analysis, it is especially illuminating when considering waves produced by a small localized disturbance, propagating through an environment with gradually varying properties. As shown first by Görtler (1943) and rediscovered by Mowbray and Rarity (1967), the oscillatory motions can then be concentrated in bands bounded by 'rays' originating at the edges of the source. Fig. 2.7 pl. II, taken from the latter paper, shows the effect in a striking way; we will return to a detailed discussion of these experiments later.

The equations (2.2.1) will be used here in the Boussinesq approximation, setting $\rho = \rho_0$, a constant. The elimination of the pressure from the first two by cross differentiation then gives

$$\frac{\partial}{\partial t}\left(\frac{\partial u}{\partial z} - \frac{\partial w}{\partial x}\right) - \frac{\partial g'}{\partial x} = 0. \tag{2.2.4}$$

This form shows that only horizontal gradients of buoyancy are responsible for changing the y-component of vorticity

$$\zeta_y = \frac{\partial u}{\partial z} - \frac{\partial w}{\partial x},$$

in agreement with the general result (1.3.5). Further differentiation

and combination of the equations can be used to eliminate g' and u to give a single equation for w,

$$\frac{\partial^2}{\partial t^2}\left(\frac{\partial^2 w}{\partial x^2}+\frac{\partial^2 w}{\partial z^2}\right)+N^2(z)\frac{\partial^2 w}{\partial x^2}=0, \tag{2.2.5}$$

in terms of which it is convenient to continue the analysis. (Of course corresponding equations can be derived for the other variables, whose solutions must have the same time and space dependence.)

Assuming a plane progressive wave solution of the form

$$w=\hat{w}(z)\exp \mathrm{i}(kx-\omega t)$$

and substituting into (2.2.5) gives for $\hat{w}$

$$\frac{\mathrm{d}^2\hat{w}}{\mathrm{d}z^2}+\left(\frac{N^2}{\omega^2}-1\right)k^2\hat{w}=0. \tag{2.2.6}$$

Instead of applying the boundary conditions round the edge of a closed region (which was the procedure used in the 'mode' approach to derive (2.2.3) for example), consider the implications of (2.2.6) when a small local disturbance is applied to the stratified fluid. The solutions of this equation only have a wave-like character when $\omega < N$; energy can then propagate away from the region where it is generated. If $\omega > N$ the disturbances remain local and fall off exponentially away from the source, and waves cannot exist. Thus the buoyancy frequency N can be interpreted as the upper limit of frequency for which wave motions can exist in a stratified fluid. In a fluid with variable N, waves will be trapped within the layer where N exceeds the imposed frequency (see (2.2.11) and the following discussion), but sharp interfaces can sustain waves of arbitrary frequency, since N is then very large.

Now let us specialize further to the case where N^2 is constant (i.e. to a linear density gradient in the Boussinesq approximation), and $\hat{w}=\overline{w}\,\mathrm{e}^{\mathrm{i}mz}$ is also periodic in z. It follows that the dispersion relation is (c.f. (2.2.3))

$$\omega=N\left(\frac{k^2}{k^2+m^2}\right)^{\frac{1}{2}}, \tag{2.2.7}$$

or

$$\omega=N\cos\theta, \tag{2.2.8}$$

where θ is the angle ($|\theta|\leqslant\frac{1}{2}\pi$) between the horizontal and the resultant wavenumber vector $\mathbf{k}$ (whose components are k and m).

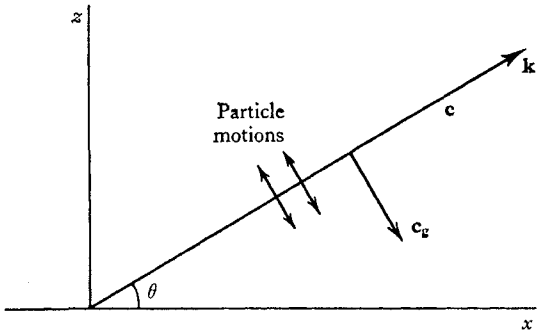

Fig. 2.8. The relation between the phase and group velocities and the particle motions for plane waves propagating through a continuously stratified fluid.

For a given stratification, therefore, waves with fixed $\omega < N$ propagate at a fixed angle to the horizontal independent of the wavelength, and this result is accurately verified by experiments of the kind shown in fig. 2.7 pl. II. The horizontal phase velocity $c_p = \omega/k$ clearly does still depend on the wavelength and hence on the scale of the phenomenon of interest.

The continuity equation implies that

$$i\mathbf{k} \cdot \bar{\mathbf{u}} = 0, \tag{2.2.9}$$

so the particle velocities are all in lines perpendicular to $\mathbf{k}$ (and parallel to the direction of the wavefronts – see fig. 2.8). For a motion of this kind the non-linear terms $\mathbf{u} \cdot \nabla \mathbf{u}$ in the equations of motion are *identically* zero, and thus a single wave component is a solution of the full equations of motion. There is now no restriction on amplitude, but nevertheless the linear theory remains applicable.

Several particular cases are of interest. When $m = 0$, $\omega = N$ and the wavefronts and particle motions are vertical; this is in accord with the original definition of N as the natural frequency of a vertically displaced particle. A similar argument can be used to show that $N \cos\theta$ is the natural frequency of a particle displaced at an angle $(\frac{1}{2}\pi - \theta)$ to the horizontal. This then gives a physical reason why special directions are so important; when a frequency is imposed externally the fluid picks out that direction of oscillation which allows it to match the forcing motion. The other limit of low

frequency (i.e. a small steady perturbation) must be such that $k^2 \ll m^2$. The motion is necessarily horizontal, and in phase over all x. In two dimensions, a solid body moved slowly in the x-direction will carry with it the layer of fluid bounded by tangent planes above and below, since there can be no vertical flow to carry fluid around it. This result (which is of course obtainable directly from the equations of motion in this limit) is analogous to the formation of 'Taylor columns' in rotating fluids, and will be referred to again in §3.3.2. (See also Veronis (1967).)

The group velocity is again significant in determining the direction of energy transfer; for waves propagating in two dimensions it has components (cf. (2.1.6))

$$\mathbf{c}_g = \left(\frac{\partial\omega}{\partial k}, \frac{\partial\omega}{\partial m}\right). \tag{2.2.10}$$

Since ω depends only on the direction of $\mathbf{k}$ and not on its magnitude (2.2.8) the group velocity must be normal to $\mathbf{k}$ and hence to the phase velocity. Energy is transmitted away from a source along rays which coincide with the directions of the particle motions; these are characteristics of the differential equation derived from (2.2.1) and lie at an angle $\sin^{-1}\omega/N$ to the horizontal (see fig. 2.8). The magnitude of $\mathbf{c}_g$ is $|\mathbf{c}_g| = (N/|\mathbf{k}|)\sin\theta$ (using the notation of (2.2.8) and fig. 2.8), with components

$$\left.\begin{aligned} u_g &= N\frac{m^2}{(k^2+m^2)^{\frac{3}{2}}} = \frac{N}{|\mathbf{k}|}\sin^2\theta, \\ w_g &= -N\frac{km}{(k^2+m^2)^{\frac{3}{2}}} = -\frac{N}{|\mathbf{k}|}\sin\theta\cos\theta. \end{aligned}\right\} \tag{2.2.11}$$

The horizontal components of $\mathbf{c}$ and $\mathbf{c}_g$ are thus directed in the same sense, while the vertical components are in opposite senses.

These ideas can be applied to fluids in which the density gradient varies slowly from point to point. One uses a method similar to that of geometrical optics, tracing the paths of rays whose directions are defined locally by (2.2.8). There are two conditions under which a group of waves can no longer propagate vertically; when either $\theta = 0$ or $\frac{1}{2}\pi$ the vertical group velocity (2.2.11) becomes zero. As $\theta \to 0$, the wavefronts are turned towards the vertical and the energy is reflected at the level where $\omega = N$, with a cusp in the ray path (fig. 2.9). Successive reflections of this kind ensure that the wave

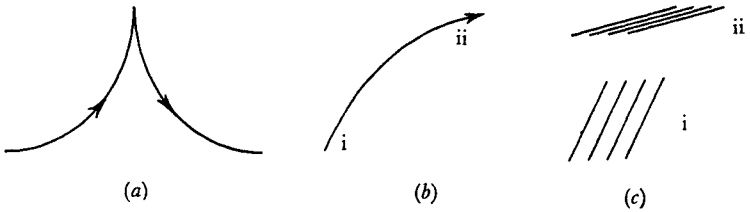

Fig. 2.9. Reflection and absorption of waves in a continuously stratified fluid. Paths of rays (*a*) in a weakening gradient, reflection where $\theta = 0$, $\omega = N$, (*b*) at a critical level, absorption when $\theta \to \frac{1}{2}\pi$, (*c*) the behaviour of a wave group in case (*b*).

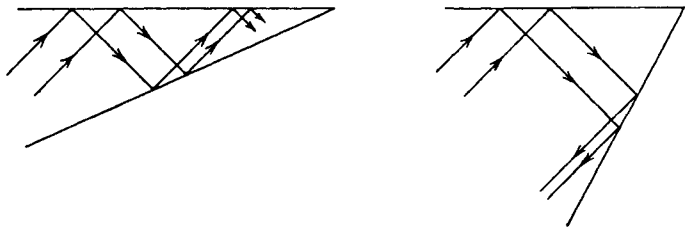

Fig. 2.10. Reflection conditions at solid boundaries. The angle which rays make with the horizontal stays constant.

energy is retained in the region where $N > \omega$ (in the ocean thermocline for example). As $\theta \to \frac{1}{2}\pi$ the wavefronts become nearly horizontal and $c_p \to 0$; this case is of special importance in a moving fluid, and will be discussed further in §2.3.3.

The reflection conditions at a solid boundary should also be mentioned here. The angle the rays make to the *horizontal* ($\frac{1}{2}\pi - \theta$) must be the same for the incident and reflected rays, since this depends only on frequency (2.2.8) regardless of the angle of the boundary β. If $\beta > \frac{1}{2}\pi - \theta$ energy will be reflected back, with the horizontal component of group velocity in the opposite direction to the incident ray, but if $\beta < \frac{1}{2}\pi - \theta$ it will continue in the same direction after reflection (fig. 2.10). For a given frequency, a shallow enough wedge acts as a perfect absorber of internal waves, since energy cannot escape backwards. From the geometry of adjoining rays, it is clear that the wavelength and velocity do change on reflection (except at vertical or horizontal boundaries) and in a wedge the wavelength will decrease and the amplitude grow. This problem has been treated in detail by Wunsch (1969), including the singular

case where $\beta = \frac{1}{2}\pi - \theta$. Eventually the waves must break and the energy is absorbed by viscous dissipation (see §4.3.4).

2.2.3. *Laboratory experiments on waves in bounded regions*

It is now possible to explain most, but not all, of the features of experiments such as that pictured in fig. 2.7 pl. II. In this section these and related observations will be described in more detail, with the additions needed to give a more complete understanding. To produce this picture Mowbray and Rarity (1967) used an elegant optical (Schlieren) technique to detect horizontal density gradients caused by the propagation of two-dimensional waves away from an oscillated cylinder. Similar patterns are seen when aluminium particles suspended in the flow are illuminated from the top (see fig. 2.11 pl. II); in that case the orientation of the particles, and the light reflected from them, is a measure of the local shear. Experiments using either of these techniques verify the main predictions of the ray theory. In a uniform density gradient, the dominant particle motions are in straight lines and confined to bands lying between rays emanating from the edges of the wavemaker, at an angle $\sin^{-1}\omega/N$ to the horizontal. Reflections from the vertical and horizontal boundaries can be seen in fig. 2.11, with a steepening of the ray paths at the top and bottom (because the condition that there can be no diffusion through a boundary reduces the density gradient to zero there, and the 'cusp' condition for reflection is approached).

One also sees in both these experiments an optical manifestation of crests and troughs (i.e. brighter and darker lines) moving across the bands, in a direction normal to the particle motion. These are clear evidence for a phase velocity in the predicted direction, but cannot be explained purely in terms of motions in phase with the plunger, which would cause the whole of a band to move as a solid plug with a shear layer at its edge. There are also seen to be smaller oscillatory motions in the regions outside the bands, and both of these effects can be described by adding a wave component which is 90° out of phase. This also allows the boundary conditions to be fitted at the wavemaker and round the whole perimeter of a closed region.

At first sight it seems inconsistent to attempt a description of a

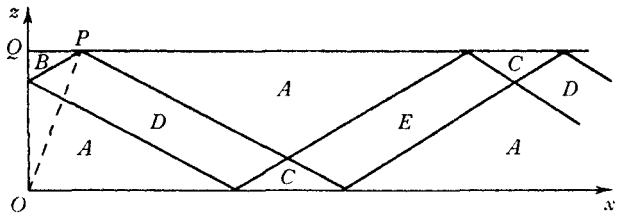

Fig. 2.13. The flow regions associated with the oscillation of a segment PQ of the boundary in a closed box (see text).

boundary value problem in terms of the ray theory, but the fact that it is possible underlines the duality of the two approaches. The mode theory emphasizes the free oscillations of a region with given fixed boundaries, whereas ray theory is appropriate when the motion is forced by oscillating part of the boundary (though the rest of the boundary may be fixed). Both features are brought out in the photograph of fig. 2.12 pl. II due to Thorpe (1968*a*). He was generating various modes in a container by oscillating a paddle at one end, but a band of strong motions propagating away from the edge of the wavemaker in accordance with ray theory is also clearly seen. Such problems with mixed boundary conditions have been solved completely in several cases: as noted above it has been done for a wedge (Wunsch 1969, Hurley 1970), for waves in a channel passing a thin vertical barrier (Larsen 1969*a* and Sandstrom 1969), and for the emission of internal waves by vibrating slender cylinders (Hurley 1969). Baines (1969) has treated the case where a section PQ of the upper boundary at one end of a semi-infinite channel is oscillated vertically (see fig. 2.13); his results will be described briefly here since they correspond closely to the experiment shown in fig. 2.11 pl. II in which the wavemaker was a solid piston.

Baines showed how the boundary conditions round the solid walls plus that of outward propagating energy towards infinity can be satisfied using a sum of internal wave modes plus a barotropic motion, all with frequency ω. The net effect of the summation varies strongly with position however. In the regions D and E (fig. 2.13) the in-phase component is a block motion along the characteristics, i.e. described by ray theory; there is vertical motion under the piston in B, and horizontal motion in C. In each of these

regions there is also an out-of-phase component, which has a logarithmic infinity at the edge of D and E because of the discontinuity in the forcing motion (which of course is removed by viscosity in a real fluid). When these two components are added, a line of no motion is found to move across the bands from left to right during a cycle, and it is this which can be observed visually and interpreted as the motion of a crest. Outside the regions covered by the beam and its reflections (i.e. in A) only the out-of-phase motion is present. Streak photography of neutrally buoyant particles has confirmed these predictions for the various regions at different phases of the cycle. A special case is worth mentioning; when the frequency is such that the characteristic from the corner of the piston at P goes to O, only the regions B and C are then present. All the internal wave modes cancel, and the barotropic mode remains, with vertical motion in B and horizontal in C, and a strong shear layer between. This motion can conveniently be produced in a channel of finite length by having a second plunger at the other end, oscillating in antiphase.

Transient problems of wave generation have also received some attention. Rarity (1967) has studied the waves produced by a two-dimensional body moving through a stratified fluid in a straight line at an arbitrary angle to the horizontal. Experiments confirming the essential predictions of this theory have been reported by Stevenson (1968), who has also considered the three-dimensional problem. Larsen (1969*b*) has observed the free oscillations of solid spheres displaced in a fluid having a constant density gradient. It is relevant to mention this here, since he can explain the measured damping of the oscillation entirely in terms of the radiated waves, with only a minor contribution to the drag coming from the viscous boundary layer.

2.3. Waves in a moving stratified fluid

2.3.1. *Velocity constant with height*

We will now discuss the additional effects which become possible when infinitesimal two-dimensional waves are propagating in a *moving* fluid with continuous stratification (though some recent developments in this subject must be left to §3.1.4, where non-linear processes are considered). When the fluid velocity is constant

with height, the first extension is a relatively simple one. Any travelling wave mode in a region bounded by a flat bottom can have a constant velocity superimposed on it; if this is chosen to be equal and opposite to the horizontal phase velocity, then another kind of stationary wave results, with fluid moving through the crests over the whole region $-\infty < x < \infty$. (The cellular wave solution (2.2.3), for example, can be extended in this way.) Of more practical importance is the generation of a stationary pattern of *lee waves* by an obstacle placed in the flow (e.g. a mountain at the bottom of the atmosphere). The choice of the proper sum of wave-like and decaying motions which satisfy the imposed boundary conditions is the problem here, and results are given below for an inviscid, Boussinesq liquid having constant N^2. Some subtle points which arise in the complex variable analysis used to obtain them will be ignored here.

Consider first a flow with velocity U confined between fixed planes a distance H apart in the vertical, containing stationary waves produced by an obstacle of (small) height h and width b placed at the origin. The phase velocity of the waves must be upstream relative to the fluid, and such that $c_p = -U$. The group velocity also has an upstream component; moreover it follows from (2.2.7) and (2.2.11) that the horizontal component of c_g is less than c_p for all possible modes trapped between $z = 0$, $z = H$, and so energy is being swept downstream. Thus the waves are indeed 'lee waves' in this situation, since no energy is available to sustain them upstream.

When the flow of interest is steady relative to fixed axes, the time derivatives in (2.2.5) may be replaced by the spatial derivatives (i.e. one can set $\mathrm{D}/\mathrm{D}t \equiv U\,\partial/\partial x$) which gives

$$U^2 \frac{\partial^2}{\partial x^2}\left(\frac{\partial^2 w}{\partial x^2} + \frac{\partial^2 w}{\partial z^2}\right) + N^2 \frac{\partial^2 w}{\partial x^2} = 0. \tag{2.3.1}$$

The linearization here depends on h/H being small, and this also implies that the boundary condition at the obstacle, which is $w = U\mathrm{d}h/\mathrm{d}x$, can be applied at $z = 0$, not on the raised obstacle itself. The other boundary conditions are $w = 0$ at $z = H$, and $w = 0$ as $x \to -\infty$ for all z; no assumption is made about w as $z \to +\infty$. From (2.3.1) one can derive an equation equivalent to

(2.2.6) for the amplitude $\hat{w}(z,k)$ of a wave with horizontal wavenumber k, namely

$$\frac{\partial^2\hat{w}}{\partial z^2}+\left(\frac{N^2}{U^2}-k^2\right)\hat{w}=0. \tag{2.3.2}$$

It is clear that any motion with $k=0$ will also satisfy (2.3.1); these modes, which are called 'columnar' because the motions are uniform in the x-direction, do not enter in the steady linear theory, but they will be referred to again in §3.1.3.

The kinds of waves which are possible in this flow can best be understood by examining the case where $\hat{w}$ is set equal to zero at $z=0$ as well as at $z=H$ (i.e. the free wave modes in the channel with the obstacle removed). The vertical velocity has non-decaying (sinusoidal) solutions satisfying these simpler top and bottom boundary conditions only for a discrete set of $k=k_n$ such that

$$(k_0{}^2-k_n{}^2)^{\frac{1}{2}}H=n\pi, \tag{2.3.3}$$

where $k_0=N/U$ and n is an integer. There is a finite number of separate wavetrains (i.e. k_n), which can exist with a given flow and stratification when there are rigid boundaries above and below. The behaviour of this system thus depends largely on the magnitude of the parameter $Ri_0=F^{-2}=k_0{}^2H^2=N^2H^2/U^2$, which has the form of an overall Richardson number (§1.4). If this is very small (e.g. U is too large for a given N), no stationary lee waves can form, since all such waves are then swept downstream. As Ri_0 increases above π^2 (or F falls below π^{-1} and the flowspeed becomes *subcritical* for the particular mode in question) first one, then two wavenumbers can satisfy (2.2.3), and so on.

These conclusions are not changed when a shallow obstacle is placed in the flow and the forced motions are of interest, but the information about its shape has not yet been used; this enters through the application of the proper boundary condition on (2.3.2), which fixes the amplitudes of all the components. As we will see again in chapter 3, for an infinitesimal obstacle the amplitude is proportional to hb, i.e. to its cross-sectional area, rather than just its height. When b is increased to finite values, the wave amplitude will be largest when k_nb is of order unity. This condition implies that the width of the obstacle is comparable with

the wavelength of one of the possible lee wave modes, thus ensuring that the forcing frequency is close to a natural frequency of the system. This can happen in the atmosphere for commonly found values of U and N^2, and some mountain ranges with just the right width to give this kind of resonant excitation of the lowest mode k_1 frequently have prominent trains of lee waves associated with them.

The atmosphere, of course, differs from the above model in that it is virtually unconfined at the top, rather than having a rigid upper lid, but the arguments can be extended to that case without difficulty. (Historically important solutions were obtained for instance by Queney (1941, 1948) and Lyra (1943) for exponential density distributions and special obstacle shapes, but these will not be discussed in detail.) Both exponentially decaying and oscillatory types of solution in z can be relevant here. The latter must always be chosen to have a form which corresponds to the *upward* propagation of energy, and if for practical reasons the calculations is cut off at some fixed upper level, this outward radiation condition must always be applied there. The continual radiation of energy upwards (which spreads it through a large volume) means that the amplitude of the waves decreases with increasing x at large distances downstream, even without friction, in contrast to the case of a rigid upper lid where the energy is reflected back and remains in the flow. In the unbounded case, the limit of (2.3.3) as $H \to \infty$ implies that lee waves should be possible for any wind speed (since $Ri_0 \to \infty$ provided $k_0 \neq 0$), but in practice lee waves are not observed if $k_0 b$ is small. Another overall Richardson number based on the dimensions of the obstacle instead of H becomes relevant and the square root of this, $\kappa = Nh/U$, is the parameter used in the non-linear theory of §3.1.4. Detailed flow patterns will be described in that section.

2.3.2. *Lee waves with varying properties in the vertical*

If the horizontal velocity u is now allowed to be a function of height z instead of constant, an extra term $w\,\partial u/\partial z$ appears in the horizontal momentum equation (2.2.1 *a*), representing the vertical convection of mean horizontal momentum by the perturbed flow. Proceeding

as before, it follows that the equation for the amplitude $\hat{w}$ (replacing (2.3.2)) is

$$\left.\begin{aligned} &\frac{\partial^2\hat{w}}{\partial z^2}+\left(\frac{N^2}{u^2}-\frac{1}{u}\frac{\partial^2 u}{\partial z^2}-k^2\right)\hat{w}=0, \\ \text{or}\quad &\frac{\partial^2\hat{w}}{\partial z^2}+(l^2(z)-k^2)\hat{w}=0 \end{aligned}\right\} \tag{2.3.4}$$

with $$l^2(z)=\frac{N^2}{u^2}-\frac{1}{u}\frac{\partial^2 u}{\partial z^2}.$$

Provided $l^2 > 0$, the behaviour is little changed by the addition of the extra term; in a flow with $\partial u/\partial z$ decreasing upwards, this just acts to increase the restoring force on a displaced particle (i.e. like an increased density gradient). In cases of practical interest the effect of allowing N also to be variable is small and so $l(z)$ can be assumed to contain this variation as well.

Much of the detailed work based on (2.3.4) has assumed for the convenience of calculation that the stratified fluid (e.g. the earth's atmosphere) can be approximated by a series of layers in which l^2 is step-wise constant, reducing the problem again to one with constant coefficients. Scorer (1949) considered two layers, the lower having depth h and $l = l_1$ and the upper very deep with $l = l_2$, and connected them by requiring both components of velocity to be continuous at the boundary. A mode analysis then showed that lee waves are possible provided

$$l_1^2-l_2^2 > \pi^2/4h^2, \tag{2.3.5}$$

i.e. provided l decreases upwards sufficiently rapidly. The waves obtained in this way have the character of an interfacial wave on the boundary between the regions, and the lower layer acts like a wave-guide along which this can propagate. (See § 2.2.2.)

Various three-layer models such as those of Scorer (1954) and Corby and Wallington (1956) have extended these ideas to find particular combinations of layer depths and l values which will lead to large lee waves amplitudes. One more recent example will be given. Pearce and White (1967) have made numerical calculations for the case of an atmosphere consisting of two layers with the same l^2, above and below a thin 'inversion' layer in which $l^2 = l_3^2$ is larger. The possible wave patterns now depend strongly on the

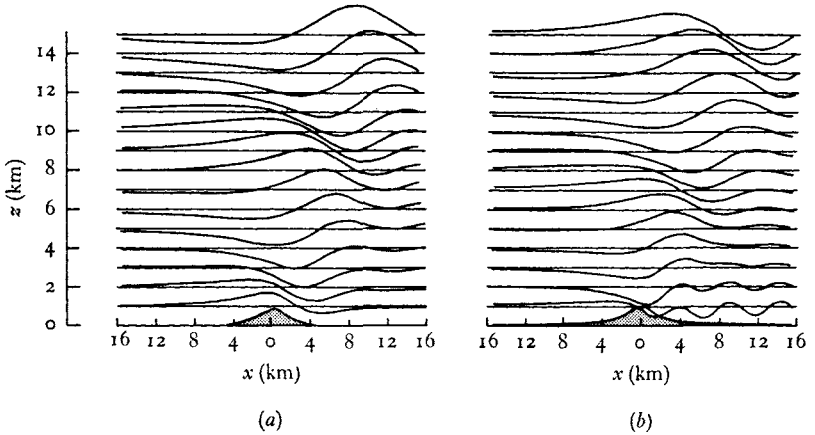

Fig. 2.14. Displacements of streamlines over a ridge, computed for (*a*) an airstream for which l^2 is nearly independent of height, (*b*) a flow for which l^2 is substantially larger in the lowest 2 km. (After Sawyer 1960. These figures are Crown copyright and are produced with the permission of the Controller of H.M.S.O.)

waveguide effect of this intermediate stable layer. For a given l_3 and barrier shape, the maximum wave amplitude near the inversion layer has a sharp maximum as a function of its depth. In the range where the amplitude decreases as the depth decreases, the wavelength of the possible waves is increasing. This is consistent with the observed behaviour of atmospheric lee waves, which weaken when the lower layers are heated, thus reducing the inversion thickness through the process of turbulent entrainment from below. (See chapter 9 for a further discussion of this last point.)

It is by no means necessary to restrict the discussion to these special and somewhat artificial variations of l^2 with height. Sawyer (1960) has computed the streamlines for the flow of observed air streams (as well as some idealized flows) over a two-dimensional barrier of the form $z = h_0/(1+(x/b)^2)$, a shape first used by Queney (1941) and incorporated in many subsequent calculations. He was able to deal numerically with continuous variations of l^2, cutting the calculation off at the top by assuming a small constant l^2 above this and using the outward radiation condition. In various circumstances he found lee waves diminishing in amplitude downstream, or staying substantially constant when there are very stable layers near the ground, and two examples are given in fig. 2.14. Note that the line of

the crests slopes backwards (against the flow) with increasing height, which is a general property of lee waves. This is consistent with a group velocity and propagation of energy relative to the fluid directed in that same sense, upstream and away from the obstacle (see § 2.2.2). Sawyer confirmed the conclusions arrived at by studying simpler models, and added more information about the behaviour at greater heights. When l^2 increases upwards, waves can maintain a large amplitude up to the stratosphere (the inertial effect of density variation i.e. the factor $(\rho_0/\rho)^{\frac{1}{2}}$ is significant here), though these may decrease in amplitude downstream. If two wavelengths are possible, the shorter is emphasized near the ground and the longer at higher levels.

It should also be noted that problems related to lee waves can arise when there is a layer of convecting fluid below a stably stratified region, rather than a solid obstacle. The large eddies of the convection may then be regarded as moving relative to the stable layer, and generating waves in it. (See §§ 7.3.4 and 9.2.4.)

2.3.3. *Reversals of velocity and critical layers*

It was implicitly assumed above in discussing (2.3.4) that $u \neq 0$, since then the equation becomes singular. When the flow velocity reverses direction with height (so that the mean horizontal velocity $u(z)$ relative to the obstacle is zero at some level), important effects arise which require separate treatment. These will be sketched using the concepts of ray theory and group velocity (§ 2.2.2), following the method used by Bretherton and Garrett (1968) and in previous work referred to by them. They have provided rigorous justification for the ray tracing procedure, and have shown that a medium may be regarded as locally uniform provided the gradient Richardson number is large and the vertical wavelength small compared to the scale of variation of U and N in the region of interest.

When fluid is moving, the frequency of a wave measured relative to a fixed point is no longer given by (2.2.7); that is the frequency relative to the fluid, but it is changed by the advection of wave crests past the point to become

$$\omega = ku \pm Nk(k^2+m^2)^{-\frac{1}{2}}. \tag{2.3.6}$$

It is this frequency which is imposed at the source and which must

remain constant following a wave group. The rate of transmission of energy relative to the fluid (i.e. the group velocity) is unchanged by the locally uniform motion so the total group velocity relative to the ground again has components $(\partial\omega/\partial k, \partial\omega/\partial m)$ and (2.2.11) are modified only by adding the local wind speed to the horizontal component.

Near a level where

$$\omega_1 \equiv \omega - ku = 0, \tag{2.3.7}$$

i.e. where the phase velocity ω/k equals the velocity of flow, the wave will not be propagating at all through the fluid; this occurs for stationary lee waves when $u = 0$ since the mechanism of their formation ensures that the phase velocity relative to the ground is zero. As such a critical level is approached, (2.3.6) shows that m must become large. The wavefronts become nearly horizontal and closer together, but in such a way that the horizontal wavenumber k is unaltered following a group. (See fig. 2.9*c*.) Both components of group velocity become zero, relative to the fluid at the critical level, and so the energy density (and amplitude of the waves) increases to large values here. This is consistent with a general result proved by Bretherton and Garrett (1968): it is no longer the energy density E, but E/ω_i which is conserved following a wave group, where ω_i (defined by (2.3.7)) is called the intrinsic frequency of the wave relative to the local mean flow. More detailed studies of the critical layer have been reported by Booker and Bretherton (1967) and Hazel (1967); these confirm that, when the gradient Richardson number is greater than about unity, very little wave energy gets through the critical level.

The consequences of this concentration of energy (and of the associated absorption of the momentum flux) will be explored further in chapters 4 and 10. It suffices to say now that the momentum lost by the waves can act to accelerate the mean flow, and there can also be instabilities associated with the increased wave amplitudes. The main predictions of this theory of the critical layer have been verified in a simple laboratory experiment (Hazel 1967). A shear flow can be produced in a long closed tube containing stratified fluid by tilting it about a horizontal axis (see chapter 4 where this method is described more fully in another context). A linear stratification produces a linear velocity profile with zero velocity at the central

depth. A small obstacle at the bottom of the flow produces lee waves, made visible in fig. 2.15 pl. IV by thin lines of dye placed at regular height intervals. In accordance with the prediction waves reach the centre of the channel but cannot pass through the level where $u = 0$. There is also the suggestion in this experiment of a distortion of the velocity profile corresponding to the injection of momentum at the critical level.

2.4. Weak non-linearities: interactions between waves

The success of linear theory in describing the various phenomena mentioned above gives confidence in the basic assumption that the component waves can be regarded as independent. If this were not so, and energy were transferred rapidly and indiscriminantly between the modes because of non-linear effects which have been omitted, no simple pattern could remain recognizable for long. There is one circumstance, however, in which even a weakly non-linear process can have an important result, and this will be described next. In this extension each individual wave can still be treated by linear theory, but when several waves satisfy certain resonance conditions, energy is interchanged preferentially between them. The other extreme case of strong non-linear interactions, where no such selective effect operates, has more of the characteristics of turbulence, and this will be discussed in later chapters and also briefly in §2.4.3.

2.4.1. *The mechanism of resonant interaction*

All interaction calculations require much tedious algebra to complete the details but the essential physical argument can be given more simply and without at first referring to a particular problem. Consider any system which can be described on linearized theory in terms of a sum of undamped waves $\sin(\mathbf{k}\cdot\mathbf{x} - \omega t)$, and for which the dispersion relation is known, say

$$F(\mathbf{k}, \omega) = 0. \tag{2.4.1}$$

Suppose now that two waves specified by $(\mathbf{k}_1, \omega_1)$ and $(\mathbf{k}_2, \omega_2)$ are of small enough amplitude for each to be adequately described in this

way, but that the lowest order cross-product term is retained. That is, the equation describing, for example, the displacement of an interface will now contain an extra term $\sin(\mathbf{k}_1 \cdot \mathbf{x} - \omega_1 t) \cdot \sin(\mathbf{k}_2 \cdot \mathbf{x} - \omega_2 t)$. This can be regarded as a forcing disturbance acting on the linearized system, and the problem of 'interaction' consists in calculating the response to this weak forcing. As for any vibrating system, the response must depend on the relation between the natural and forcing frequencies.

Now the above product (forcing) term can be expressed as sum and difference waves with wavenumbers and frequencies

$$\left.\begin{aligned} \mathbf{k}_3 &= \mathbf{k}_1 \pm \mathbf{k}_2, \\ \omega_3 &= \omega_1 \pm \omega_2. \end{aligned}\right\} \tag{2.4.2}$$

Each combination having one of the wavenumbers $\mathbf{k}_3$ will tend to generate secondary waves which are possible free modes of the system, that is, which have frequencies ω_j satisfying $F(\mathbf{k}_3, \omega_j) = 0$, and move with the phase speed $\omega_j/|\mathbf{k}_3|$. In general none of the ω_j will equal ω_3 given by (2.4.2), and so the forcing and the secondary waves will not remain in phase and the energy transfer will remain small. If, on the other hand, $\omega_3 = \omega_j$ and one of the combination waves moves at the same speed as a free oscillation of the same wavenumber, resonance occurs; the waves stay in phase and a continuous transfer of energy can take place. The growth is limited by the amount of energy available in the primary waves, by the closeness of ω_3 and ω_j and by viscosity in a real fluid. Other factors which influence the time during which $\mathbf{k}_1$ and $\mathbf{k}_2$ overlap (such as the length of the wavetrains) are also relevant, but given long enough, such secondary waves can grow to amplitudes comparable with those of the primary waves, no matter how small the original amplitude.

This process, in which two waves interact to give a third, is called a *quadratic interaction*, and three waves which are related by (2.4.2) and separately satisfy the dispersion relation (2.4.1) constitute a *resonant trio*. If there are no other transfers, the energy in such a trio is just passed back and forth among the components (since the mechanism still operates if another pair of waves is regarded as primary). In some special cases the variations of all three components have been calculated explicitly as functions of time. It is a property of the weak interaction process that the period characteristic of the

interchange is much longer than those of the separate wave components, and this period is inversely proportional to the amplitude of the interacting waves (Bretherton 1964). For a lucid general treatment of this problem, see Simmons (1969).

It should be noted that the wavenumbers used above are vector wavenumbers, and so in general waves travelling in different directions can interact. Hasselman (1966) has shown how a wide variety of resonant interaction processes can be conveniently discussed by constructing vector diagrams which are closely related to collision diagrams for elementary particles, but none of these more sophisticated results will be given here.

2.4.2. *Interactions of interfacial waves*

Particular examples of resonant interactions can now be given, starting with the simple case of interfacial waves in a two layer system studied by Ball (1964). He showed that the conditions for resonance can be satisfied by a triplet consisting of two surface waves $(\mathbf{k}_1, \omega_1)$, $(\mathbf{k}_2, \omega_2)$ travelling in opposite directions, and an interfacial wave $(\mathbf{k}_3, \omega_3)$ having the same direction as one of them. One such triplet is shown diagrammatically by the points AB_1C_1 on the dispersion curves drawn in fig. 2.16. The two branches of the curve are just equations (2.1.7) for the internal mode and (2.1.8) for the surface mode, with particular choices of the density difference and layer depths. For two-dimensional waves this and a similar triplet AB_2C_2 are the only possible ones involving wave A. When a general direction of propagation is allowed, however, wave A can interact with an infinite set of other surface waves (two for each choice of direction) and the result must again be an internal wave.

Herein lies the relevance of this process for internal waves, and the reason why it has been mentioned although surface waves *per se* are not of concern to us here. It is a possible mechanism for generating internal waves from surface waves on the ocean, which can operate over a wide range of conditions of the surface. It is especially significant when compared with purely surface gravity wave interactions, since Phillips (1960) has shown that those can only occur at higher order, between three components to give a fourth (i.e. that no

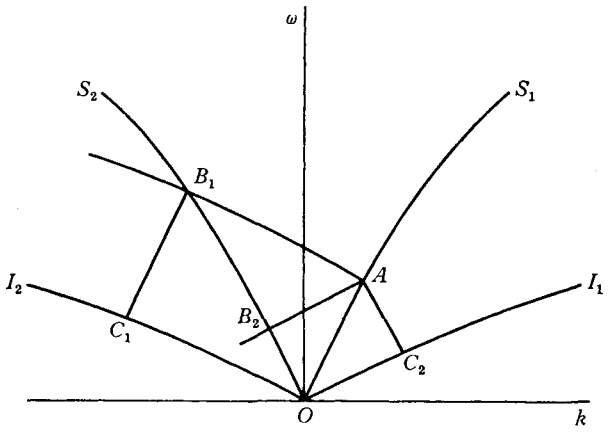

Fig. 2.16. Schematic representation of the conditions for resonant interaction. The surface wave A belongs to the two interacting wave triplets $A\,B_1\,C_1$ and $A\,B_2\,C_2$. (From Ball 1964.)

resonant *trio* can be found using only one branch of the dispersion curve or surface).

The locus of surface wavenumbers of arbitrary direction, which can interact with a given wavenumber to give an internal wave, is shown in fig. 2.17 for two choices of the frequencies ω_1 and ω_2. As the difference in frequency (and therefore $\omega_3 = \omega_2 - \omega_1$, the frequency of the internal wave) becomes small, the distance between the two branches of this curve is reduced. Thus as shown by the vectors on the right-hand figure, one can get an interaction between two surface waves of nearly the same wavenumber (but different directions) to produce an internal wave of comparable wavenumber in a third direction, having the very low frequency characteristic of internal waves. It is also clear from this vector diagram that short waves travelling in nearly the same direction can interact to produce a much longer (smaller $|\mathbf{k}|$) wave, travelling nearly at right angles to the surface waves. The attenuation of the disturbances with depth should be least important in this latter case, and significant long waves on a shallow thermocline can arise even though the surface wave motions themselves fall off sharply with depth (see Thorpe (1966*b*) for a more detailed discussion of this problem).

No direct experimental demonstration of this surface–internal wave interaction has been given (experimenters have been deterred

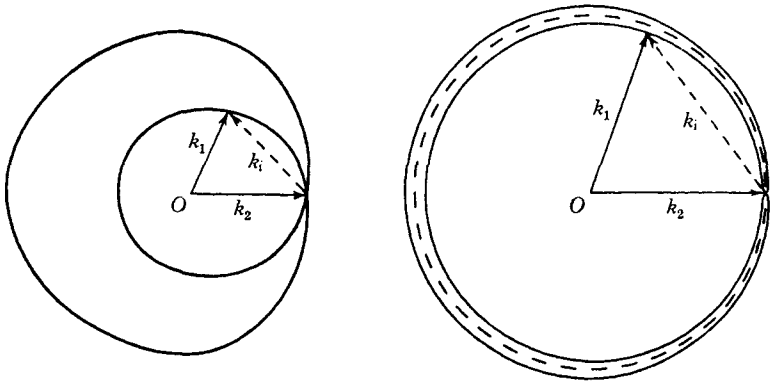

(*a*) (*b*)

Fig. 2.17. Loci of surface vector wavenumbers $\mathbf{k}_1$ which can interact resonantly with $\mathbf{k}_2$ to give an internal wavenumber $\mathbf{k}_i$. The magnitudes of $\mathbf{k}_1$ and $\mathbf{k}_2$ are (*a*) unequal (*b*) nearly equal.

by the difficulties of absorbing the surface waves without disturbing the stratification). A comparable interaction has, however, been demonstrated between three wave modes all on the interfacial transition region separating two uniform layers. Davis and Acrivos (1967*b*) observed that a simple waveform generated at one end of a channel can under certain circumstances become unstable, in the sense that irregularities characteristic of higher modes spontaneously appear on the interface. (See fig. 2.18 pl. III.) They explained this behaviour by showing that resonant triads can exist for which the two waves interacting with the primary wave can begin with arbitrarily small amplitude, and both grow exponentially by extracting energy from the primary wave. (Hasselman (1967) showed that this is an example of a more general result, namely that the sum interaction of the pair described by (2.4.2) will always be unstable in this way.)

This can be illustrated by writing down the equations for the variation of amplitudes in the general form

$$\left.\begin{aligned} \mathrm{d}a_1/\mathrm{d}t &= \alpha_1 a_2 a_3, \\ \mathrm{d}a_2/\mathrm{d}t &= \alpha_2 a_3 a_1, \\ \mathrm{d}a_3/\mathrm{d}t &= \alpha_3 a_1 a_2. \end{aligned}\right\} \qquad (2.4.3)$$

Here the α_i are the interaction constants (whose calculation for

particular systems will not be undertaken). Suppose that $a_1 = A$ is so much larger than a_2 and a_3 that initially it can be regarded as constant. Then (2.4.3) can be linearized and have solutions

$$a_2, a_3 \sim \exp\{\pm A\sqrt{(\alpha_2\alpha_3)}\,t\}. \tag{2.4.4}$$

In a real fluid, the growth will be limited also by viscosity, and adding damping terms proportional to amplitude gives

$$\left.\begin{aligned} \mathrm{d}a_2/\mathrm{d}t &= \alpha_2 A a_3 - \beta_2 a_2, \\ \mathrm{d}a_3/\mathrm{d}t &= \alpha_3 A a_2 - \beta_3 a_3. \end{aligned}\right\} \tag{2.4.5}$$

(For a discussion of the calculation of the coefficients β_2 and β_3 and other effects of viscosity see, for example, Thorpe (1968*c*).) Thus growth is possible provided $\alpha_2\alpha_3 > 0$ and

$$A > A_{\mathrm{crit}} \equiv (\beta_2\beta_3/\alpha_2\alpha_3)^{\frac{1}{2}}. \tag{2.4.6}$$

Davis and Acrivos applied these results to the wave modes on a density profile of the form $\rho \propto \tanh(z/L)$ (some more details will be given in §4.3.3). They showed that the above conditions for growth can be satisfied by a trio consisting of a primary wave, the second mode moving in the same direction (the simplest description of the observed bulges on the interface shown in fig. 2.18) and a third mode component travelling in the opposite direction, which could be produced by reflections at the far end of the experimental tank. The measured relation between the frequencies agreed with that predicted from the dispersion relations using the observed interface thickness. They also showed that the critical amplitude criterion can be translated into a frequency condition, for fixed amplitude of the primary wave. Instability will only occur provided the frequency ω_1 is high enough, and a thick interface is more unstable than a thin one, for a given density difference. All of these statements are in agreement with their own experimental findings, and with some earlier observations reported by Keulegan and Carpenter (1961) which were at that time unexplained.

2.4.3. *Interactions with continuous stratification*

Thorpe (1966*b*) has generalized the arguments outlined above to include interactions which occur between internal wave modes with either multilayered or continuous stratification. The only restriction

is that not all the waves of a resonant trio can belong to the same mode (for the same reason as purely surface wave quadratic interactions are excluded). Phillips (1968) combined the frequency condition for resonance ($\omega_3 = \omega_1 \pm \omega_2$) with the result (2.2.8) for bodily internal waves. Together these imply that the slopes of the three interacting wavenumbers to the horizontal must form a closed triangle

$$\cos\theta_1 \pm \cos\theta_2 = \cos\theta_3 \tag{2.4.7}$$

and this geometrical property can be used with the summation condition on the wavenumbers to construct diagrams of the possible interactions with a given internal wave. Interactions between waves and currents can be included by regarding the latter as the limit of a wave as $\omega \to 0$ (Phillips, George and Mied 1968). It has been shown, for example, how periodic variations of density or current speed can lead to the trapping of internal waves in a finite layer of an unbounded fluid, essentially by a resonance mechanism.

Direct observations of a resonant interaction between three internal wave modes in a linearly stratified fluid have been made in a large laboratory channel by Martin, Simmons and Wunsch (1969). They produced the first and third modes using an array of paddles to give appropriate independent displacements at one end of the tank, and absorbed the energy at the other end using a 'beach' in the form of a shallow wedge having a small enough angle not to reflect any of the frequencies of interest (see §2.2.2 and Wunsch 1969). They tuned the paddle frequencies close (but not exactly) to the resonant condition and measured vertical displacements by means of conductivity probe arrays at various depths and distances from the wavemaker.

They found, in agreement with theory, that a fourth mode wave could be detected by numerical analysis of the spectra and cross spectra of the signals from the vertical arrays. Its amplitude grows not with time but with distance down the channel (because this determines how long the waves have been interacting) and its phase velocity is in the opposite direction to that of the original two. This mode is clearly distinguished in the periodograms because it has a much larger amplitude than any other peak corresponding to sums or differences of the original frequencies. There is also evidence of

multiple resonances leading to higher modes, which have been more thoroughly documented in later experiments.

McEwan (1971) has reported an elegant experiment in which a resonant interaction was observed between a trio of standing internal waves in a rectangular tank of linearly stratified salt solution. One mode (generally that having one half wavelength in the vertical direction and a few wavelengths in the horizontal) was directly forced, together with its harmonics. Two higher free modes then grew from the background noise, each energized by the interaction of the other with the forced wave. The results are in excellent agreement with a theory developed for the standing wave case, and this configuration seems especially suitable for careful quantitative work. Viscous dissipation round the boundaries and due to the internal shears can be estimated accurately, and the amplitude of forcing necessary to produce growing disturbances to the original mode can readily be calculated (cf. (2.4.6)). McEwan was particularly interested in the processes of degeneration of the wave field and wave breaking at supercritical amplitudes, but a discussion of this aspect of his work will have more relevance in the context of mixing in the interior of large bodies of stratified fluid, and will therefore be deferred until the final chapter.

Before we leave the subject of weak resonant interactions they should be contrasted again with strong interactions, in this context of a continuously stratified fluid. The fact that each wave mode separately satisfies the equations of motion exactly has already been mentioned (following (2.2.9)), and this implies that the amplitudes can become large, while the non-linear terms in the equations of motion still vanish identically. It is now possible for forced modes, generated by an arbitrary pair of internal waves of large amplitude, to attain amplitudes comparable with the primary waves without the help of the resonance mechanism. These can in turn interact with each other and with the original internal wave modes with no restrictions on frequency or wavenumber, and instead of energy being interchanged continuously and slowly between three modes, the result will be an indiscriminant transfer of energy between many modes.

The formal statement of the conditions for each of these mechanisms can be expressed in several equivalent ways (Phillips 1966*a*,

p. 178), which physically amount to the following. The resonant mechanism is the more important provided the vorticity associated with the internal waves remains small compared to the buoyancy frequency N, and this restriction also ensures that the interaction must extend over many wave periods for substantial transfer of energy. If on the other hand a typical rate of vertical shear (which is usually the more important contribution to the vorticity) is of the same order as N

$$\partial u'/\partial z \sim N, \tag{2.4.8}$$

(i.e. the gradient Richardson number (1.4.3) is of order one or less), then the forced modes are comparable in magnitude to the initial modes and they can develop rapidly within a period of the primary wave. The condition for a range of a continuous spectrum near wavenumber magnitude k to have a vigorous ('turbulent') energy exchange can be written in a form comparable to (2.4.8), namely

$$S \equiv \{k^3 E(k)\}^{\frac{1}{2}} \sim N, \tag{2.4.9}$$

and weak resonant interactions are important when $S \ll N$. This is the appropriate generalization of (2.4.8) since the combination on the left is the only quantity with the dimensions of a shear which can be formed from k and the energy density $E(k)$. (See § 5.2.2 for the definition of $E(k)$ and a further discussion of this point.)